Bloch mode scattering matrix methods for modeling extended photonic crystal structures. I. Theory

L. C. Botten,[1,*] T. P. White,[2] A. A. Asatryan,[1] T. N. Langtry,[1] C. Martijn de Sterke,[2] and R. C. McPhedran[2]
[1]*Centre for Ultrahigh-Bandwidth Devices for Optical Systems (CUDOS) and Department of Mathematical Sciences, University of Technology, Sydney, Broadway New South Wales 2007, Australia*
[2]*Centre for Ultrahigh-Bandwidth Devices for Optical Systems (CUDOS) and School of Physics, University of Sydney, Sydney, New South Wales 2006, Australia*
(Received 8 April 2004; published 15 November 2004)

We present a rigorous Bloch mode scattering matrix method for modeling two-dimensional photonic crystal structures and discuss the formal properties of the formulation. Reciprocity and energy conservation considerations lead to modal orthogonality relations and normalization, both of which are required for mode calculations in inhomogeneous media. Relations are derived for studying the propagation of Bloch modes through photonic crystal structures, and for the reflection and transmission of these modes at interfaces with other photonic crystal structures.

DOI: 10.1103/PhysRevE.70.056606 PACS number(s): 42.70.Qs, 42.25.Fx, 42.79.Dj

I. INTRODUCTION

Photonic crystals (PCs) have become one of the mainstream research areas in contemporary optics [1]. This interest is fueled by the unique, intrinsic properties of such structures which resemble, in some respects, those of semiconductors. It has already been established that photonic crystals have the ability to guide light along intricate paths without substantial diffraction losses [2]. Photonic crystal materials can also modify substantially the electromagnetic density of states [3] leading to their ability to control the emission properties of sources embedded in them. In particular, they can completely suppress the density of states, thus creating a “true vacuum” for electromagnetic waves. These capabilities are ideally suited to the miniaturization of optical components leading to ultracompact optical devices that can be assembled onto a single photonic chip [4], and already an all-optical transistor based on the photonic crystal has been proposed [5]. Different components inside a photonic chip may be connected using complicated “wiring” networks comprising waveguides with bends [6], Y [7] and T junctions [8], channel drop filters [9], as well as different types of directional couplers [10,11]. In such complex microstructures, photonic crystals with different parameters (such as superprisms [12] or Mach-Zehnder interferometers [13]) may be interfaced. The modeling of such devices thus requires a comprehensive understanding of how PC devices couple to one another or to external conventional waveguides [14], and how light is guided within such devices.

The modeling of photonic crystals and composite devices built from these is a challenging task. The choice of optical materials and the geometry and scale of the structure makes the PC a strongly scattering environment in which it is necessary to take into account many scattering events. Among the numerical methods that are generally used to model PC structures are finite difference time domain methods [15], plane-wave methods [16], beam propagation methods [17], transfer matrix methods [18], layer Korringa-Kohn-Rostoker methods [19,20], Wannier function methods [21,22], and finite element methods [23].

Although these methods often produce accurate results, they are entirely numerical in their approach and do not easily give physical insight into the underlying propagation mechanisms. Despite the importance of this, thus far only an approximate semianalytic theory based on coupled mode analysis has appeared in Refs. [24,25]. Recently, methods based on the Bloch mode transfer matrix, or related techniques, have emerged and generated interest [22,26–34]. We have used the transfer matrix formalism in our method and developed a semianalytic approach to the modeling of photonic crystals based on the Bloch mode expansion. While a brief account of our method has been presented [33,34], this paper provides a comprehensive treatment of the method, and of its underlying mathematical structure, which reveals the limitations of the coupled mode method [24,25].

The real strength of the method is its use of the natural (Bloch mode) basis of functions to describe the properties of photonic crystals. If we consider a plane wave incident upon a photonic crystal, the incident field excites a field within the PC which can be expanded as a superposition of Bloch modes. In many practical situations, however, only one or, more generally, a few propagating Bloch states actually contribute to the far field of the device. This reduces the complexity of the analysis of the multiple scattering problem and, in many cases, transforms the analysis of the PC to that of well known devices (such as generalizations of the Fabry-Pérot interferometer) that arise in thin-film optics.

The paper is divided into two parts: Part I provides the rigorous theoretical foundation using the complete set of modes while in Part II [35] we study a range of applications including waveguide dislocations, resonators, folded directional couplers, and coupled Y junctions, the calculations for which use both the complete mode set and also expansions that are appropriately truncated.

In Part I, we begin in Sec. II by establishing the Bloch mode basis for a two-dimensional (2D) photonic crystal from

*Electronic address: Lindsay.Botten@uts.edu.au

the solution of an algebraic eigenvalue problem associated with the transfer matrix. We then characterize the modes via constraints imposed on the transfer matrix by reciprocity and, for lossless structures, energy conservation. Each of these imposes a pairing relationship which enables the set of all modes to be partitioned into downward and upward sets, with otherwise identical sets of propagation constants. These conservation relationships also allow us to normalize and orthogonalize the modes, which subsequently enable modal field quantities to be expressed in their physically most intuitive form. In Sec. III, we analyze propagation in extended photonic crystal devices by studying the basic building blocks: propagation in a single (finite or infinite) uniform PC medium, and the scattering and diffraction of Bloch modes at a single interface between two semi-infinite PCs. With respect to the latter, the action of the interface is characterized in terms of Bloch mode reflection and transmission scattering matrices that are generalizations of the Fresnel coefficients in thin-film optics. Finally, the extended structure is modeled in a recursive manner that exploits the two basic building blocks described immediately above. In the companion article, Part II [35], which deals with a range of applications, we also study the asymptotics of far field calculations and justify the use of only the propagating Bloch modes in that case.

II. BLOCH MODES AND THEIR CHARACTERIZATION

A. Method and nomenclature

We consider a two-dimensional structure that comprises a set of stacks $M_1, M_2, \ldots, M_N$, each of which is built from identical diffraction grating layers with a transverse period D_x. Media M_1 and M_N are semi-infinite and represent the input and output domains for the problem. While M_1 and M_N may be photonic crystals, they may also be any homogeneous medium (e.g., dielectric or free space), or more generally any periodic medium (provided that the periods of all media are common) for which Bloch modes can be defined. Because of the gratings' periodicity, the functional elements of the structure are contained within a supercell (see Fig. 1), the dimension of which is chosen to be large enough to ensure effective isolation from neighboring supercells when operated within a band gap of the bulk crystal.

The periodicity imposed by the diffraction grating model means that individual layers are coupled together by plane-wave diffraction orders, the directions θ_s of which are given by the grating equation

$$k \sin \theta_s = \alpha_s = \alpha_0 + \frac{2\pi s}{D_x}, \quad s = 0, \pm 1, \pm 2, \ldots, \tag{1}$$

where $\alpha_0 = k_{0x}$ is the component of the Bloch vector along the direction of periodicity of the gratings, and $k = 2\pi/\lambda$ is the wave vector in the background medium. The integers s in Eq. (1) run over a finite set of propagating orders, and an infinite set of evanescent orders.

In a PC, the action of each grating is determined not only by its geometry, but also by the geometry of the lattice in which it is embedded. In general, four scattering matrices—

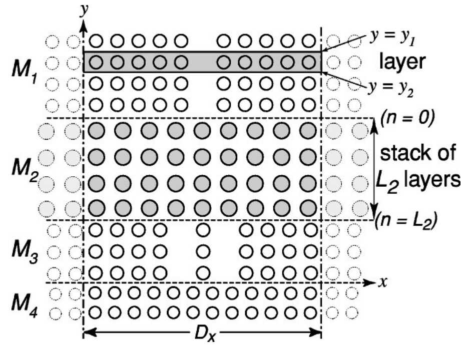

FIG. 1. Schematic of a photonic crystal structure formed by joining stacks (M_1–M_N) (here $N=4$), each consisting of identical grating layers. All layers must have the same supercell period D_x, but the positions and properties of the cylinders within a layer can all be different. Stacks M_2–M_{N-1} contain L_m layers; stacks M_1 and M_N are semi-infinite. Layer interfaces within each stack are numbered $n=0$ to L_m.

two for reflection and two for transmission—are required since each grating may appear differently when viewed from above or below. We note that for a simple (up-down symmetric) cylinder grating embedded in a rectangular lattice, the symmetry of both the cylinder and the lattice enables the grating to be characterized by a single reflection and a single transmission matrix. In the treatment that follows, we denote the plane-wave reflection and transmission scattering matrices of a single layer by $\tilde{\mathbf{R}}, \tilde{\mathbf{T}}$ and $\tilde{\mathbf{R}}', \tilde{\mathbf{T}}'$, with the two pairs corresponding to incidence from above and below, respectively. For example, the element $\tilde{R}_{pq}$ specifies the reflected amplitude in plane-wave order p due to unit amplitude incidence from above in plane-wave order q. The tilde is used here to differentiate between the plane-wave scattering matrices for a single grating layer, and those for a grating stack, which we introduce in Sec. III.

Grating scattering matrices can be computed with a variety of techniques, including integral equation methods and differential-Fourier methods [31,32,36,37], among others. Here, however, we use a *multipole* method [20], which is appropriate to cylinder gratings, and which is an efficient computational tool. The sole proviso on the use of this method is that adjacent layers do not interpenetrate, thus allowing the use of plane-wave field expansions (3) at matching interfaces. Strictly speaking, the requirement that layers do not interpenetrate is sufficient, but not necessary. In fact, provided that the interpenetration is not too severe, the plane-wave expansions on the matching interfaces are still valid. The issue is directly related to the Rayleigh controversy of diffraction grating theory [37] concerning the validity of plane-wave representations for outgoing fields within the grooves of diffraction gratings. In cases where layer interpenetration is a problem, it is necessary to abandon the multipole method as the means of computing the scattering matrices, replacing it by alternative techniques including differential (Fourier), integral, or finite element methods.

For the cases to which it applies, the multipole method is arguably the preferred technique as the formulation is analytically elegant, and structurally embodies key properties

[38] such as reciprocity and energy conservation analytically within the formulation. These properties can be verified (effectively) to within machine precision and the analytic preservation of these properties is inherited by the Bloch modes, making the method both analytically tractable and easy to validate numerically.

Here we introduce the eigenvalue problem defined by the transfer matrix and proceed in subsequent sections to classify the modes, and to derive important results that are used to normalize and orthogonalize modes. These are needed in order to provide a suitable basis for field amplitude and energy calculations that realizes the key properties of reciprocity and energy conservation in the most simple and elegant manner.

We begin by considering an infinite 2D photonic crystal, operated in either of its two fundamental polarizations. In the background medium, the fields satisfy the usual Helmholtz equation

$$(\nabla^2 + k^2)V(\mathbf{r}) = 0 \tag{2}$$

where k denotes the wave number in the background medium. In the cases of TM and TE polarizations, respectively the scalar function V denotes the single electric and magnetic field component that is aligned with the axis of the cylinders. On the the upper and lower interfaces (respectively denoted by $j=1$, 2 in Fig. 1) of a grating layer, we expand the fields in plane waves as

$$V_f^{(j)}(\mathbf{r}) = \sum_{s=-\infty}^{\infty} \chi_s^{-1/2}(f_s^{(j)-}e^{-i\chi_s(y-y_j)} + f_s^{(j)+}e^{i\chi_s(y-y_j)})e^{i\alpha_s x}, \tag{3}$$

where α_s is defined in Eq. (1), $\chi_s=\sqrt{k^2-\alpha_s^2}$, with $\mathrm{Im}(\chi_s)\geqslant 0$, and the y_j are the heights of the reference interfaces (see Fig. 1). While such plane-wave expansions are strictly valid only for noninterpenetrating layers, the solution for interpenetrating layers may be constructed by envisaging infinitesimal thickness interfaces of background material, separating the grating layers, in which these plane-wave expansions are valid. Accordingly, we characterize the plane-wave fields at the interfaces j by vectors of plane-wave coefficients of the form $\mathbf{f}^{(j)\mp}=[f_s^{(j)\mp}]$, associated with the subscript and superscript entries in the field term $V_f^{(j)}(\mathbf{r})$.

In the design of PC devices, the entire structure is generally operated in a band gap. The use of a plane-wave method thus necessitates that the lateral size D_x of the supercell be sufficiently large to isolate device components. Provided D_x is large enough, this isolation renders the calculation essentially independent of the value of α_0. For convenience, the reasons for which become apparent later, we choose $\alpha_0=0$.

The transfer matrix [26,28] relates the fields $\mathbf{f}_j$ on either side of the grating according to the relation

$$\mathbf{f}_2 = \boldsymbol{\mathcal{T}}\mathbf{f}_1 \text{ where } \boldsymbol{f}_j = \begin{bmatrix} \boldsymbol{f}^{(j)-} \\ \mathbf{f}^{(j)+} \end{bmatrix}, \tag{4}$$

and

$$\begin{aligned}\boldsymbol{\mathcal{T}} &= \begin{bmatrix} \tilde{\mathbf{T}} - \tilde{\mathbf{R}}'\tilde{\mathbf{T}}'^{-1}\tilde{\mathbf{R}} & \tilde{\mathbf{R}}'\tilde{\mathbf{T}}'^{-1} \\ -\tilde{\mathbf{T}}'^{-1}\tilde{\mathbf{R}} & \tilde{\mathbf{T}}'^{-1} \end{bmatrix} \\ &= \begin{bmatrix} \tilde{\mathbf{T}} & \tilde{\mathbf{R}}' \\ \mathbf{0} & \boldsymbol{I} \end{bmatrix}\begin{bmatrix} \boldsymbol{I} & \mathbf{0} \\ \tilde{\mathbf{R}} & \tilde{\mathbf{T}}' \end{bmatrix}^{-1} \\ &\overset{\text{def}}{\equiv} \boldsymbol{\mathcal{U}}_2\boldsymbol{\mathcal{U}}_1^{-1}. \end{aligned} \tag{5}$$

The matrices $\boldsymbol{\mathcal{U}}_1$ and $\boldsymbol{\mathcal{U}}_2$ have a simple physical interpretation, relating the total field vectors $\mathbf{f}_j$ on either side of the grating layer to the incoming fields impinging upon the grating. That is,

$$\mathbf{f}_1 = \boldsymbol{\mathcal{U}}_1\mathbf{f}_{\text{inc}}, \quad \mathbf{f}_2 = \boldsymbol{\mathcal{U}}_2\mathbf{f}_{\text{inc}} \text{ where } \mathbf{f}_{\text{inc}} = \begin{bmatrix} \boldsymbol{f}^{(1)-} \\ \boldsymbol{f}^{(2)+} \end{bmatrix}. \tag{6}$$

The Bloch modes of the crystal then follow from the imposition of the Bloch condition which leads to the eigenvalue equation

$$\boldsymbol{\mathcal{T}}\mathbf{f} = \mu\mathbf{f}, \tag{7}$$

where $\mu=\exp(-i\mathbf{k}_0\cdot\mathbf{e}_2)$, $\mathbf{e}_i$ denotes the basis vectors of the lattice formed by the gratings, and $\mathbf{k}_0=(k_{0x},k_{0y})$ is the Bloch vector with $k_{0x}=\alpha_0=0$, as described above. Here, $\mathbf{e}_2$ is the basis vector in the direction of translation.

While the transfer matrix $\boldsymbol{\mathcal{T}}$ is of fundamental theoretical importance, it is of limited practical computational use because of the numerical problems that arise in the computation of the inverse of the transmission matrices $\tilde{\mathbf{T}}'$. Instead, the eigenvalue problem is solved by transforming it to more robust forms [27,28].

Any practical solution requires the truncation of the infinite plane wave series (3), resulting in transfer matrices of even dimension. It is then possible to partition the solutions of Eq. (7) into equal numbers of downward and upward propagating modes, with the actual nature of the pairing discussed in Sec. II B. For the present, we observe that for nonpropagating states ($|\mu|\neq 1$), which carry no energy through an infinite crystal, their directionality is characterized by the direction of their decay—downward $|\mu|<1$, and upward $|\mu|>1$. The directionality of the propagating states $|\mu|=1$ is characterized by the vertical component of group velocity v_{gy} of the mode. Since the group velocity and the energy flux $(\mathcal{E}_f)$ normal to the grating are related by $\mathcal{E}_f \propto v_{gy}\mathcal{E}_D$ (where $\mathcal{E}_D$ is the energy density), it follows that modal directionality can be inferred from the sign of the mode flux $\mathcal{E}_f$ [26], with positive and negative values, respectively, denoting downward and upward propagation [38]. Here,

$$\mathcal{E}_f = \mathbf{f}^H\boldsymbol{\mathcal{I}}_{\text{PW}}\mathbf{f} = \boldsymbol{f}_-^H\mathbf{I}_p\boldsymbol{f}_- - \boldsymbol{f}_+^H\boldsymbol{I}_p\boldsymbol{f}_+ - i(\boldsymbol{f}_-^H\boldsymbol{I}_{\bar{p}}\boldsymbol{f}_+ - \boldsymbol{f}_+^H\boldsymbol{I}_{\bar{p}}\boldsymbol{f}_-), \tag{8}$$

where

$$\boldsymbol{\mathcal{I}}_{\text{PW}} = \begin{bmatrix} \boldsymbol{I}_p & -i\boldsymbol{I}_{\bar{p}} \\ i\boldsymbol{I}_{\bar{p}} & -\boldsymbol{I}_p \end{bmatrix}, \tag{9}$$

with $\boldsymbol{I}_p$ denoting a diagonal matrix whose rows and columns designate the plane-wave (PW) channels and whose values are 1 for propagating (i.e., nonevanescent) plane waves (χ_s real) and 0 otherwise. $\boldsymbol{I}_{\bar{p}}=\boldsymbol{I}-\boldsymbol{I}_p$ is its complement, containing unit diagonal elements only for the evanescent plane waves.

With the modes now partitioned, $\mathcal{T}$ can be written in its diagonalized form

$$\mathcal{T}=\mathcal{F}\mathcal{L}\mathcal{F}^{-1}, \tag{10}$$

a result that encapsulates the entire family of eigenvalue equations $\mathcal{T}\mathcal{F}=\mathcal{F}\mathcal{L}$ from Eq. (7). In this representation, $\mathcal{F}$ is a matrix, the columns of which are the eigenvectors of $\mathcal{T}$, and $\mathcal{L}$ is a diagonal matrix whose entries are the corresponding eigenvalues μ. In the light of the eigenvalue pairings discussed above, we may partition $\mathcal{F}$ and $\mathcal{L}$ as follows:

$$\mathcal{F}=\begin{bmatrix} \boldsymbol{F}_- & \boldsymbol{F}'_- \\ \boldsymbol{F}_+ & \boldsymbol{F}'_+ \end{bmatrix}, \quad \mathcal{L}=\begin{bmatrix} \boldsymbol{\Lambda} & \boldsymbol{0} \\ \boldsymbol{0} & \boldsymbol{\Lambda}' \end{bmatrix} \tag{11}$$

with the columns of the matrices $\boldsymbol{F}_\mp, \boldsymbol{F}'_\mp$ formed from the $\boldsymbol{f}_\mp$ components of the eigenvectors for the downward and upward modes, respectively, and with $\boldsymbol{\Lambda}$ and $\boldsymbol{\Lambda}'$ being diagonal matrices containing the corresponding eigenvalues μ_j for the downward and upward propagating states. For convenience, the modes are ordered with propagating modes, i.e., those for which $|\mu_j|=1$, listed first.

B. Mode characterization: Reciprocity and symplecticity

Important results that characterize the modes may be derived from the physical concepts of reciprocity and energy conservation. In this section we focus on the former, a geometrical constraint that holds for any nonmagnetic material, and show that it constrains the transfer matrix to be symplectic and enforces a pairing of downward and upward states.

The derivation follows from the application of Green's theorem

$$\iint (V_g\nabla^2 V_f - V_f \nabla^2 V_g)dA = \oint \left(V_g \frac{\partial V_f}{\partial n} - V_f \frac{\partial V_g}{\partial n}\right) ds \tag{12}$$

around the supercell grating layer. The fields V_f and V_g both satisfy the Helmholtz equation with the same value of k. On the interfaces $j=1$, 2 of Fig. 1 (above and below the grating layer) the fields are represented by plane-wave expansions (3) associated with vectors of field coefficients. Since the area integral in Eq. (12) vanishes and the field periodicity ($\alpha_0=0$) cancels contributions to the line integral at the edges of the supercell, it follows that the line integrals $I_R(y)$ over the upper and lower surfaces Γ_j, $j=1$, 2, are identical. That is, $I_R(y_1)=I_R(y_2)$ where

$$I_R(y_j)=\frac{1}{2iD_x}\int_0^{D_x} \left(V_g\frac{\partial V_f}{\partial y} - V_f \frac{\partial V_g}{\partial y}\right)\bigg|_{y=y_j} dx = \mathbf{g}_j^T \mathcal{Q}_{\mathrm{PW}} \mathbf{f}_j, \tag{13}$$

with

$$\mathcal{Q}_{\mathrm{PW}}=\begin{bmatrix} \boldsymbol{0} & \boldsymbol{Q} \\ -\boldsymbol{Q} & \boldsymbol{0} \end{bmatrix}. \tag{14}$$

Here, $\mathcal{Q}_{\mathrm{PW}}$ denotes the reversing permutation which is derived by reversing the order of the rows of the identity matrix $\boldsymbol{I}$. In Eq. (13), the fields represented by $\mathbf{g}_j$ and $\mathbf{f}_j$ are both plane-wave series of the form (3), for the same value of k, the coefficients of which are the entries of the respective vectors. The relevant generalized inner product (13), in bilinear form in this problem, is skew symmetric, i.e., $\mathbf{g}_j^T\mathcal{Q}_{\mathrm{PW}}\mathbf{f}_j=-\mathbf{f}_j^T\mathcal{Q}_{\mathrm{PW}}\mathbf{g}_j$, mirroring the properties of the cross product which is inherited from Maxwell's curl equations. Note that the choice of $\alpha_0=0$ ensures that the plane-wave basis in which V_f and V_g are expanded is common to both and also orthogonal, thus leading to the bilinear form in Eq. (13).

Thus, the skew-symmetric inner product $\mathbf{g}^T\mathcal{Q}_{\mathrm{PW}}\mathbf{f}$ is conserved in that it has the same value on each grating interface, i.e.,

$$\mathbf{g}_1^T\mathcal{Q}_{\mathrm{PW}}\mathbf{f}_1=\mathbf{g}_2^T\mathcal{Q}_{\mathrm{PW}}\mathbf{f}_2. \tag{15}$$

Applying the transfer equations $\mathbf{g}_2=\mathcal{T}\mathbf{g}_1$ and $\mathbf{f}_2=\mathcal{T}\mathbf{f}_1$, it then follows that

$$\mathbf{g}_1^T(\mathcal{T}^T\mathcal{Q}_{\mathrm{PW}}\mathcal{T}-\mathcal{Q}_{\mathrm{PW}})\mathbf{f}_1=0.$$

Observing that $\mathbf{f}_1$ and $\mathbf{g}_1$ may be expressed in terms of the incoming fields $\mathbf{f}_{\mathrm{inc}}$ and $\mathbf{g}_{\mathrm{inc}}$ via $\mathbf{f}_1=\mathcal{U}_1\mathbf{f}_{\mathrm{inc}}$ and $\mathbf{g}_1=\mathcal{U}_1\mathbf{g}_{\mathrm{inc}}$, we deduce

$$\mathbf{g}_{\mathrm{inc}}^T\mathcal{U}_1^T(\mathcal{T}^T\mathcal{Q}_{\mathrm{PW}}\mathcal{T}-\mathcal{Q}_{\mathrm{PW}})\mathcal{U}_1\mathbf{f}_{\mathrm{inc}}=0. \tag{16}$$

Then, since the incident fields may be chosen arbitrarily and $\mathcal{U}_1$ is nonsingular, we deduce that $\mathcal{T}$ must be symplectic [39]—a common nomenclature for the result

$$\mathcal{T}^T\mathcal{Q}_{\mathrm{PW}}\mathcal{T}=\mathcal{T}\mathcal{Q}_{\mathrm{PW}}\mathcal{T}^T=\mathcal{Q}_{\mathrm{PW}},$$

$$\text{or } \mathcal{T}^T=\mathcal{Q}_{\mathrm{PW}}\mathcal{T}^{-1}\mathcal{Q}_{\mathrm{PW}}^{-1}, \tag{17}$$

with respect to the generalized inner product (13) defined in terms of the skew-symmetric matrix $\mathcal{Q}_{\mathrm{PW}}$ (14). This symplectic structure is a natural reflection of the reciprocity theorem and holds even when material losses are present.

Since $\mathcal{T}^T$ and $\mathcal{T}^{-1}$ are related by a similarity transformation (17), the eigenvalues of $\mathcal{T}^T$, namely, μ, and the eigenvalues of $\mathcal{T}^{-1}$, namely, μ^{-1}, must be paired. In particular, if μ is the eigenvalue of a downward propagating state, then μ^{-1} is the eigenvalue of the corresponding upward propagating state. From this it follows that eigenvalue matrices $\boldsymbol{\Lambda}$ and $\boldsymbol{\Lambda}'$ of Eq. (10) are related by $\boldsymbol{\Lambda}'=\boldsymbol{\Lambda}^{-1}$.

Some aspects of the structure of the eigensystem emerge when the diagonalized form of $\mathcal{T}$ (10) is applied to the symplectic property of $\mathcal{T}$ (17) to derive

$$\mathcal{L}\mathcal{F}^T\mathcal{Q}_{\mathrm{PW}}\mathcal{F}\mathcal{L}=\mathcal{F}^T\mathcal{Q}_{\mathrm{PW}}\mathcal{F}.$$

Observing that $\mathcal{F}^T\mathcal{Q}_{\mathrm{PW}}\mathcal{F}$ is antisymmetric and that $\boldsymbol{\Lambda}'=\boldsymbol{\Lambda}^{-1}$, it is easily shown that

$$\mathcal{F}^T\mathcal{Q}_{\mathrm{PW}}\mathcal{F} = \begin{bmatrix} \mathbf{0} & \boldsymbol{I} \\ -\boldsymbol{I} & \mathbf{0} \end{bmatrix} = \mathcal{Q}_{BM}, \tag{18}$$

after scaling the columns of $\mathcal{F}$ appropriately. Here $\mathcal{Q}_{BM}$ is the Bloch mode equivalent of the matrix $\mathcal{Q}_{\mathrm{PW}}$ which was defined with respect to the plane-wave basis.

Key reciprocity relations for the constituent grating layer may also be derived when we substitute Eq. (5) into Eq. (17), thus deriving $\mathcal{U}_2^T\mathcal{Q}_{\mathrm{PW}}\mathcal{U}_2 = \mathcal{U}_1^T\mathcal{Q}_{\mathrm{PW}}\mathcal{U}_1$. When all four matrix partitions of this expression are expanded, we arrive at the reciprocity relations for the scattering matrices of the single grating layer, namely,

$$\tilde{\mathbf{R}}^T = \boldsymbol{Q}\tilde{\mathbf{R}}\boldsymbol{Q}, \quad \tilde{\mathbf{R}}'^T = \boldsymbol{Q}\tilde{\mathbf{R}}'\boldsymbol{Q}, \quad \tilde{\mathbf{T}}'^T = \boldsymbol{Q}\tilde{\mathbf{T}}\boldsymbol{Q}. \tag{19}$$

As mentioned, the relationships (19) hold analytically within the multipole formulation that is used to compute the scattering matrices [38]. The symplectic nature of $\mathcal{T}$, and the eigenvalue pairing (18) that follows from this, are thus satisfied independently of the multipole truncation limits of the code that generates the scattering matrices. Therefore, Eqs. (17) and (18) hold to within (effectively) machine precision in our computational implementation. We conclude by observing that with alternative methods of computing the grating layer scattering matrices, specifically those that do not analytically conserve the relationships in Eq. (19), we may exploit these relationships as tests of the convergence of the computational method.

C. Mode characterization: Energy conservation and orthogonality

In Sec. II B, we used the geometrical constraint of reciprocity to investigate the structure of the transfer matrix associated with the eigensystem of Eq. (7). Here we further explore the properties of the eigensystem, demonstrating that energy conservation and modal orthogonality relations hold analytically within the formulation.

For lossless systems, Green's theorem

$$0 = \oiint (V_f\nabla^2\overline{V_g} - \overline{V_g}\nabla^2 V_f)dA = \oint \left(V_f\frac{\partial \overline{V_g}}{\partial n} - \overline{V_g}\frac{\partial V_f}{\partial n}\right)ds \tag{20}$$

yields a further conservation relation that establishes orthogonality relationships for the modes. Note that the left hand side of Eq. (20) vanishes only for lossless systems and that field periodicity cancels contributions to the line integral at the edges of the supercell. It thus follows that the line integrals $I_F(y)$ over the upper and lower interfaces Γ_j, $j=1$, 2, are identical. That is, $I_F(y_1)=I_F(y_2)$ where

$$I_F(y_j) = \frac{1}{2iD_x}\int_0^{D_x}\left(V_f\frac{\partial \overline{V_g}}{\partial y} - \overline{V_g}\frac{\partial V_f}{\partial y}\right)\Bigg|_{y=y_j} dx = \mathbf{g}_j^H\mathcal{I}_{\mathrm{PW}}\mathbf{f}_j, \tag{21}$$

with $\mathcal{I}_{\mathrm{PW}}$ defined in Eq. (9). The bilinear form $\mathbf{g}^H\mathcal{I}_{\mathrm{PW}}\mathbf{f}$ in Eq. (21) is simply a generalization of the energy flux of Eq. (8), with the downward flux of the plane-wave field $(\mathcal{E}_F=\mathbf{f}_j^H\mathcal{I}_{\mathrm{PW}}\mathbf{f}_j)$ corresponding to Eq. (21) with $\mathbf{g}_j=\mathbf{f}_j$.

The conservation of $I_F(y)$ on each interface implies

$$\mathbf{g}_1^H\mathcal{I}_{\mathrm{PW}}\mathbf{f}_1 = \mathbf{g}_2^H\mathcal{I}_{\mathrm{PW}}\mathbf{f}_2, \tag{22}$$

and this together with the transfer relations $\mathbf{f}_2=\mathcal{T}\mathbf{f}_1$ and $\mathbf{g}_2=\mathcal{T}\mathbf{g}_1$ yields

$$\mathbf{g}_1^H(\mathcal{T}^H\mathcal{I}_{\mathrm{PW}}\mathcal{T} - \mathcal{I}_{\mathrm{PW}})\mathbf{f}_1^H = 0.$$

Proceeding as for Eq. (16) and expressing $\mathbf{f}_1$ and $\mathbf{g}_1$ in terms of incident fields $\mathbf{f}_{\mathrm{inc}}$ and $\mathbf{g}_{\mathrm{inc}}$ which may be chosen arbitrarily, we determine a new conservation relation for the transfer matrix, namely,

$$\mathcal{T}^H\mathcal{I}_{\mathrm{PW}}\mathcal{T} = \mathcal{I}_{\mathrm{PW}}. \tag{23}$$

While relationships of this type have appeared in the literature associated with electron conductance in thin wires [40,41], this electromagnetic form differs significantly from the electronic form through the presence of the terms denoted by $\boldsymbol{I}_{\bar{p}}$ in the off-diagonal partitions of $\mathcal{I}_{\mathrm{PW}}$ (9). Such terms characterize contributions to energy related quantities arising from evanescent (nonpropagating) plane-wave order coupling.

Explicit forms for the energy conservation relations that are satisfied by the grating reflection and transmission matrices may be found by substituting the representation $\mathcal{T}=\mathcal{U}_2\mathcal{U}_1^{-1}$ (6) for the transfer matrix into Eq. (23), thus deriving

$$\mathcal{U}_2^H\mathcal{I}_{\mathrm{PW}}\mathcal{U}_2 = \mathcal{U}_1^H\mathcal{I}_{\mathrm{PW}}\mathcal{U}_1.$$

By expanding all four partitions of this matrix relation we derive

$$\tilde{\mathbf{R}}^H\boldsymbol{I}_p\tilde{\mathbf{R}} + \tilde{\mathbf{T}}^H\boldsymbol{I}_p\tilde{\mathbf{T}} = \boldsymbol{I}_p + i\tilde{\mathbf{R}}^H\boldsymbol{I}_{\bar{p}} - i\boldsymbol{I}_{\bar{p}}\tilde{\mathbf{R}}, \tag{24a}$$

$$\tilde{\mathbf{R}}^H\boldsymbol{I}_p\tilde{\mathbf{T}}' + \tilde{\mathbf{T}}^H\boldsymbol{I}_p\tilde{\mathbf{R}}' = i\tilde{\mathbf{T}}^H\boldsymbol{I}_{\bar{p}} - i\boldsymbol{I}_{\bar{p}}\tilde{\mathbf{T}}', \tag{24b}$$

$$\tilde{\mathbf{R}}'^H\boldsymbol{I}_p\tilde{\mathbf{T}} + \tilde{\mathbf{T}}'^H\boldsymbol{I}_p\tilde{\mathbf{R}} = i\tilde{\mathbf{T}}'^H\boldsymbol{I}_{\bar{p}} - i\boldsymbol{I}_{\bar{p}}\tilde{\mathbf{T}}, \tag{24c}$$

$$\tilde{\mathbf{R}}'^H\boldsymbol{I}_p\tilde{\mathbf{R}}' + \tilde{\mathbf{T}}'^H\boldsymbol{I}_p\tilde{\mathbf{T}}' = \boldsymbol{I}_p + i\tilde{\mathbf{R}}'^H\boldsymbol{I}_{\bar{p}} - i\boldsymbol{I}_{\bar{p}}\tilde{\mathbf{R}}', \tag{24d}$$

which are succinctly summarized in the form

$$\mathcal{S}^H\begin{bmatrix} \boldsymbol{I}_p & \mathbf{0} \\ \mathbf{0} & \boldsymbol{I}_p \end{bmatrix}\mathcal{S} = \begin{bmatrix} \boldsymbol{I}_p & \mathbf{0} \\ \mathbf{0} & \boldsymbol{I}_p \end{bmatrix} + i\mathcal{S}^H\begin{bmatrix} \boldsymbol{I}_{\bar{p}} & \mathbf{0} \\ \mathbf{0} & \boldsymbol{I}_{\bar{p}} \end{bmatrix} - i\begin{bmatrix} \boldsymbol{I}_{\bar{p}} & \mathbf{0} \\ \mathbf{0} & \boldsymbol{I}_{\bar{p}} \end{bmatrix}\mathcal{S}, \tag{25}$$

where

$$\mathcal{S} = \begin{bmatrix} \tilde{\mathbf{R}} & \tilde{\mathbf{T}}' \\ \tilde{\mathbf{T}} & \tilde{\mathbf{R}}' \end{bmatrix} \tag{26}$$

denotes the S matrix of the grating layer. Since these relationships hold analytically within the framework of the multipole formulation [38], Eqs. (24), and all properties that follow from these, hold analytically, independent of the truncation of the multipole series for field quantities in the determination of the scattering matrices. Equations (23)–(25)

can therefore be verified numerically, effectively to within machine precision.

We now use Eq. (23) to establish the orthogonality relations for the Bloch modes. Recall that in Sec. II B we showed that the eigenvalues μ and μ^{-1} were paired because of the symplecticity of $\mathcal{T}$ (17). A further eigenvalue pairing relationship can now be established from Eq. (23), $\mathcal{T}^H = \mathcal{I}_{\mathrm{PW}}\mathcal{T}^{-1}\mathcal{I}_{\mathrm{PW}}^{-1}$, which reveals that $\mathcal{T}^H$ and $\mathcal{T}^{-1}$ are related by a similarity transformation. Thus, for lossless systems for which Eq. (23) holds, the eigenvalues $\bar{\mu}$ and μ^{-1} are also paired, where the overbar denotes the complex conjugate. Combing this with the pairing implied by the symplectic property (17) of $\mathcal{T}$, we see that the eigenvalues of $\mathcal{T}$ always occur as a quadruple comprising $\mu, \bar{\mu}, \mu^{-1}, \bar{\mu}^{-1}$. For propagating modes (for which $\bar{\mu}=\mu^{-1}$) or evanescent modes for which μ may be real (as may occur for rectangular lattices), this quadruple degenerates to a simple pairing relationship.

The structure of the eigensystem and the nature of the orthogonality relations then follows by substituting the diagonalized form for $\mathcal{T}$ (10) into (23) to reveal

$$\bar{\mathcal{L}}\mathcal{F}^H\mathcal{I}_{\mathrm{PW}}\mathcal{F}\mathcal{L} = \mathcal{F}^H\mathcal{I}_{\mathrm{PW}}\mathcal{F}, \tag{27}$$

noting also that $\mathbf{\Lambda}' = \mathbf{\Lambda}^{-1}$ from the discussion above. Then, observing that $\mathcal{F}^H\mathcal{I}_{\mathrm{PW}}\mathcal{F}$ is Hermitian, and writing

$$\mathcal{F}^H\mathcal{I}_{\mathrm{PW}}\mathcal{F} = \begin{bmatrix} \boldsymbol{A} & \boldsymbol{B} \\ \boldsymbol{B}^H & \boldsymbol{D} \end{bmatrix}, \tag{28}$$

it follows, by expanding the partitioned form (27), that $\bar{\mathbf{\Lambda}}\boldsymbol{A}\mathbf{\Lambda}=\boldsymbol{A}$, $\bar{\mathbf{\Lambda}}\boldsymbol{B}\mathbf{\Lambda}^{-1}=\boldsymbol{B}$, and $\bar{\mathbf{\Lambda}}^{-1}\boldsymbol{D}\mathbf{\Lambda}^{-1}=\boldsymbol{D}$. From the first of these identities we see that that this requires $A_{lm}(\bar{\mu}_l\mu_m-1)=0$ for all l,m. Since $|\mu_l|=1$ for propagating states and $|\mu_l|<1$ for evanescent states, we can see that the elements A_{lm} can take nonzero values only on that part of the diagonal of the matrix $(l=m)$ that corresponds to propagating modes. Furthermore, since $\boldsymbol{A}$ is Hermitian, these diagonal entries must be real and thus we write $\boldsymbol{A}=\boldsymbol{A}_m$, indicating that the matrix has a diagonal form with nonzero entries associated with the propagating modes. The same arguments lead us to deduce that $\boldsymbol{D}$ takes the same form, i.e., $\boldsymbol{D}=\boldsymbol{D}_m$. Finally, for $\boldsymbol{B}$, we see that its elements must satisfy $\boldsymbol{B}_{lm}(\bar{\mu}_l/\mu_m-1)=0$. Since the eigenvalues μ_l occur in the quadruple discussed above, we can make the term $(\bar{\mu}_l/\mu_m-1)$ vanish by selecting l and m such that $(\bar{\mu}_l)=\mu_m$. Since the μ_l are chosen from the set of downward propagating modes, this constraint can be satisfied only for evanescent modes. Furthermore, by expanding the left hand side of Eq. (28), we see that $\boldsymbol{B}$ must be skew Hermitian and we deduce that $\boldsymbol{B}=-i\boldsymbol{B}_{\bar{m}}$ where $\boldsymbol{B}_{\bar{m}}$ is a real block diagonal matrix with nonzero entries associated only with the evanescent or nonpropagating modes. Thus,

$$\mathcal{F}^H\mathcal{I}_{\mathrm{PW}}\mathcal{F} = \begin{bmatrix} \boldsymbol{A}_m & -i\boldsymbol{B}_{\bar{m}} \\ i\boldsymbol{B}_{\bar{m}} & \boldsymbol{D}_m \end{bmatrix}. \tag{29}$$

Combining both Eqs. (18) and (29), and scaling the columns of $\mathcal{F}$ appropriately, we can write down the normalized relationships satisfied by the modes (which comprise the columns of $\mathcal{F}$)

$$\mathcal{F}^T\mathcal{Q}_{\mathrm{PW}}\mathcal{F} = \begin{bmatrix} \mathbf{0} & \boldsymbol{I} \\ -\boldsymbol{I} & \mathbf{0} \end{bmatrix} = \mathcal{Q}_{\mathrm{BM}}, \tag{30a}$$

$$\mathcal{F}^H\mathcal{I}_{\mathrm{PW}}\mathcal{F} = \begin{bmatrix} \boldsymbol{I}_m & -i\boldsymbol{I}_{\bar{m}} \\ i\boldsymbol{I}_{\bar{m}} & -\boldsymbol{I}_m \end{bmatrix} = \mathcal{I}_{\mathrm{BM}}. \tag{30b}$$

In Eqs. (30), the m subscripts refer to the propagating Bloch modes in medium m, whereas $\bar{m}$ refers to nonpropagating Bloch modes, and

$$\boldsymbol{I}_{m;n_1,n_2} = \begin{cases} \delta_{n_1n_2} & \text{for propagating states } n_1, \\ 0 & \text{otherwise}, \end{cases}$$

$$\boldsymbol{I}_{\bar{m};n_1n_2} = \begin{cases} 0 & \text{if } n_1 \text{ or } n_2 \text{ denotes a propagating state}, \\ 1 & \text{if } n_1=n_2 \text{ and } n_1 \text{ denotes an evanescent state with a real eigenvalue}, \\ \begin{bmatrix} 0 & 1 \\ 1 & 0 \end{bmatrix} & \text{if } n_1 \text{ and } n_2 \text{ are a conjugate evanescent pair}. \end{cases}$$

Observe that relations (30a) and (30b) involve all possible modes—both propagating and evanescent. We now consider the implications of *orthogonality relations* (30b) by what these reveal for individual propagating or evanescent states. Specifically, for two downward modes $\mathbf{f}_l$ and $\mathbf{f}_m$, we have $\mathbf{f}_l^H\mathcal{I}_{\mathrm{PW}}\mathbf{f}_m=\delta_{lm}$ if both are propagating and $\mathbf{f}_l^H\mathcal{I}_{\mathrm{PW}}\mathbf{f}_m=0$ for all other combinations of propagating and evanescent modes. In particular, we note that the zero diagonal elements associated with the evanescent modes imply that such modes carry zero flux. Similarly, for two upward propagating states $\mathbf{f}_l'$ and $\mathbf{f}_m'$, we have $\mathbf{f}_l'^H\mathcal{I}_{\mathrm{PW}}\mathbf{f}_m'=-\delta_{lm}$ if both are propagating and $\mathbf{f}_l'^H\mathcal{I}_{\mathrm{PW}}\mathbf{f}_m'=0$ for all other combinations. The most interesting and unusual of these relations are those associated with the evanescent coupling of a downward and an upward mode. Here we see that with $\mathbf{f}_l$ and $\mathbf{f}_m'$, respectively, denoting downward and upward propagating states, $\mathbf{f}_l^H\mathcal{I}_{\mathrm{PW}}\mathbf{f}_m'=-i\delta_{lm}$ if both modes are evanescent, and $\mathbf{f}_l^H\mathcal{I}_{\mathrm{PW}}\mathbf{f}_m'=0$ for all other combinations.

In Sec. III, we develop models for propagation in multilayer PC devices, deriving expressions for various energy quantities and developing relationships based on reciprocity and energy conservation that are used to validate the formalism. The use of an appropriately normalized modal basis is of paramount importance and the relations (30a), which expresses the normalization imposed by reciprocity, and (30b), which constitutes the orthogonality relations, are precisely the forms that are needed to ensure the representation of physical quantities, such as field amplitudes and modal fluxes, in their simplest and physically most amenable forms. With the modal basis normalized according to Eq. (30b), we can express mode fluxes in a manner that is structurally identical to that which applies to plane waves [see Eq. (35)] and which, in the simplest case, corresponds to computing the square magnitude of a modal amplitude. Furthermore, the normalization of Eq. (30a) enables all reciprocity relations for modal scattering matrices to be expressed in terms of simple matrix symmetry relations [e.g., Eq. (51)].

In concluding this section, it is important that we differentiate clearly between the orthogonality relations developed here and the more familiar orthogonality relationships that are satisfied by the modes of the operator eigenvalue equation [43]

$$\Theta\mathbf{H}(\mathbf{r}) = \nabla \times \left(\frac{1}{\varepsilon(\mathbf{r})}\nabla \times \mathbf{H}(\mathbf{r})\right) = \frac{\omega^2}{c^2}\mathbf{H}(\mathbf{r}). \qquad (31)$$

In computing the modes from the eigenvalue problem of Eq. (31), the eigenvalues of which are the permissible frequencies ω of the modes, we select a Bloch vector $\boldsymbol{k}_0$ and determine a basis of modes, the orthogonality of which follows from the Hermitian property of the operator Θ. In contrast, in our derivations above, we select the frequency (or wavelength), and solve the eigenvalue problem for the transfer matrix (7) to determine the Bloch vectors of the modes. This set of modes is complete and forms a basis in which we can expand electromagnetic fields. However, as is evident from the discussion and derivation above, these modes are not orthogonal in the conventional sense, due to the presence of the matrix $\mathcal{I}_{\mathrm{PW}}$ (9) in the defining inner product $\boldsymbol{g}^H\mathcal{I}_{\mathrm{PW}}\boldsymbol{f}$ that derives from flux considerations (21). While the matrix $\mathcal{I}_{\mathrm{PW}}$ is Hermitian, it is not positive definite (having distinct eigenvalues of ± 1) and thus cannot define a true inner product. Moreover, it is the off-diagonal blocks of $\mathcal{I}_{\mathrm{PW}}$ that are associated with paired evanescent order propagation of energy which preclude the existence of an orthogonality relationship that is analogous to those satisfied by Hermitian operators. While the orthogonality relationships derived above are important for the normalized representation of field quantities, they do not assist in the computational solution of the field problem which requires the inversion of dense matrices.

III. PROPAGATION IN PHOTONIC CRYSTAL DEVICES

This section focuses on the solution of propagation problems in extended photonic crystal devices comprising a number of PC stacks $M_1, M_2, \ldots, M_N$, as in Fig. 1. It commences with the formulation of the problem in a single PC medium and then analyzes the propagation of Bloch modes across an interface between two semi-infinite PC media, introducing Bloch mode scattering matrix generalizations of the usual Fresnel reflection and transmission coefficients. These two threads are then drawn together to solve the propagation problem in a multi-layer structure. The tools derived in Sec. II are exploited to derive elegant forms for the reciprocity and energy conservation relations.

A. Propagation in a single photonic crystal medium

We consider the propagation of light in a medium comprising L layers of a finite photonic crystal structure. We derive expressions for the plane-wave fields at successive interfaces between the grating layers $(n=0,1,\ldots,L)$ (see Fig. 1) in terms of the Bloch mode expansions, and derive an

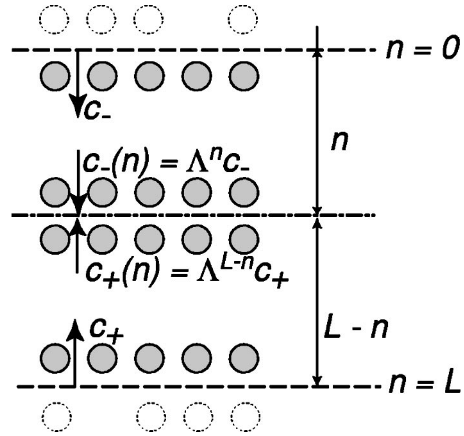

FIG. 2. Downward and upward Bloch mode amplitudes $\boldsymbol{c}_-(n)$ and $\boldsymbol{c}_+(n)$ defined at interface n in a stack of length L in terms of Bloch modes sourced, respectively, from the interfaces above $(\boldsymbol{c}_-)$ and below $(\boldsymbol{c}_+)$ the stack.

expression for the energy flux in terms of Bloch mode coefficients. Knowledge of these plane-wave quantities enables the calculation of the energy flux through the layer and the reconstruction of the field within the layer. For the multipole method that we use to generate the grating scattering matrices, a knowledge of the incoming plane-wave fields to each grating layer enables the calculation of the multipole source coefficients [20] for the cylinder grating. From this, the total field can be computed as the superposition of the incoming plane-wave fields and the outgoing scattered field expressed in a multipole series.

From Fig. 2, the interfaces $n=0$ and $n=L$ denote the boundaries between this photonic crystal stack and some other medium (such as another PC, free space, dielectric, etc.). These surfaces are respectively sources of forward (downward) and backward (upward) propagating modes respectively. At some interface n, the coefficient vectors for the downward and upward plane-wave fields used in the expansion (3) are

$$\mathbf{f}(n) = \begin{bmatrix} \boldsymbol{f}_-(n) \\ \boldsymbol{f}_+(n) \end{bmatrix} = \begin{bmatrix} \boldsymbol{F}_- \\ \boldsymbol{F}_+ \end{bmatrix}\mathbf{c}_-(n) + \begin{bmatrix} \boldsymbol{F}'_- \\ \boldsymbol{F}'_+ \end{bmatrix}\mathbf{c}_+(n) \qquad (32)$$

where $\boldsymbol{c}_\mp(n)$ denote the amplitudes of the downward and upward Bloch modes at interface n as in Fig. 2, and $\boldsymbol{c}(n) = [\boldsymbol{c}_-(n)^T \boldsymbol{c}_+(n)^T]^T$. Since the downward and upward Bloch modes travel n and $L-n$ layers, respectively, from their sources at the upper and lower boundaries, $\boldsymbol{c}_-(n) = \boldsymbol{\Lambda}^n \boldsymbol{c}_-$ and $\boldsymbol{c}_+(n) = \boldsymbol{\Lambda}^{L-n}\boldsymbol{c}_+$, where $\boldsymbol{c}_\mp$ denote the amplitudes of the downward and upward Bloch modes at their origins (Fig. 2). Hence,

$$\mathbf{f}(n) = \mathcal{F}\mathbf{c}(n), \qquad (33)$$

where

$$\mathbf{c}(n) = \mathcal{L}(L,n)\tilde{\mathbf{c}},$$

$$\mathcal{L}(L,n) = \begin{bmatrix} \Lambda^n & \mathbf{0} \\ \mathbf{0} & \Lambda^{L-n} \end{bmatrix}, \quad \tilde{\mathbf{c}} = \begin{bmatrix} \boldsymbol{c}_-(0) \\ \boldsymbol{c}_+(L) \end{bmatrix} = \begin{bmatrix} \boldsymbol{c}_- \\ \boldsymbol{c}_+ \end{bmatrix}. \quad (34)$$

Once the Bloch mode coefficients coefficients $\boldsymbol{c}_-$ and $\boldsymbol{c}_+$ are known, then $\boldsymbol{f}(n)$ can be computed for each interface, thus enabling the field within each layer to be reconstructed from a knowledge of the incoming fields [i.e., $\boldsymbol{f}_-(n), \boldsymbol{f}_+(n+1)$].

We turn now to the energy flux carried by the Bloch modes which, at each interface, is given by Eq. (8):

$$\begin{aligned}\mathcal{E}_f(n) &= \mathbf{f}^H(n)\mathcal{I}_{\mathrm{PW}}\mathbf{f}(n) \\ &= \mathbf{c}(n)^H\mathcal{F}^H\mathcal{I}_{\mathrm{PW}}\mathcal{F}\mathbf{c}(n) \\ &= \mathbf{c}(n)^H\mathcal{I}_{\mathrm{BM}}\mathbf{c}(n),\end{aligned} \quad (35)$$

where the final simplification relies on the modal orthogonality relationship (30b) and yields the Bloch mode equivalent of the plane-wave flux expression (8). Expanding this expression, we see that the energy flux at interface n is given by

$$\begin{aligned}\mathcal{E}_f(n) = \sum_{j\in\Omega_m} [|\boldsymbol{c}_-(n)_j|^2 - |\boldsymbol{c}_+(n)_j|^2] - i\sum_{j\in\Omega_{\overline{m}}} [\overline{\boldsymbol{c}_-}(n)_j\boldsymbol{c}_+(n)_j \\ - \overline{\boldsymbol{c}_+}(n)_j\boldsymbol{c}_-(n)_j],\end{aligned} \quad (36)$$

where Ω_m is the set of propagating modes, and $\Omega_{\overline{m}}$ is the set of nonpropagating or evanescent modes. The first sum in Eq. (36), over the propagating modes, is the difference between the modal fluxes for the downward and upward propagating states. Note that the normalization imposed through Eq. (30b) enables propagating mode fluxes to be computed directly from the square magnitude of the modal amplitude. The second series is a sum over the evanescent modes and expresses the flux contribution due to coupling between the downward and upward evanescent states.

We return now to the calculation of the flux in our L-layer medium and substitute $\mathbf{c}(n) = \mathcal{L}(L,n)\tilde{\mathbf{c}}$ from Eq. (33) into Eq. (35) to derive

$$\begin{aligned}\mathcal{E}_f(n) &= \tilde{\mathbf{c}}^H\overline{\mathcal{L}}(L,n)\mathcal{I}_{\mathrm{BM}}\mathcal{L}(L,n)\tilde{\mathbf{c}} \\ &= [\tilde{\boldsymbol{c}}_-{}^H \tilde{\boldsymbol{c}}_+{}^H]\begin{bmatrix} \boldsymbol{I}_m & -i\boldsymbol{I}_{\overline{m}}\Lambda^L \\ i\Lambda^L\boldsymbol{I}_{\overline{m}} & -\boldsymbol{I}_m \end{bmatrix}\begin{bmatrix} \tilde{\boldsymbol{c}}_- \\ \tilde{\boldsymbol{c}}_+ \end{bmatrix}.\end{aligned} \quad (37)$$

As expected, the flux is independent of the layer n, a result which relies on the eigenvalue pairings, discussed in Sec. II B, which constrain the eigenvalues to be real or to appear in conjugate pairs. Note also that as the length L of the medium increases, the influence of the evanescent order coupling diminishes since the evanescent states have eigenvalues $|\mu|<1$. Accordingly, for an infinitely long structure (i.e., $L\to\infty$), Eq. (37) reduces to $\Sigma_{m\in\Omega_m}|\tilde{\mathbf{c}}_m{}^-|^2 - |\tilde{\mathbf{c}}_m{}^+|^2$, the difference between the downward and upward fluxes with the summation taken over only the propagating states. Thus, in this limit, the evanescent mode pairs can carry no power.

B. Coupling semi-infinite photonic crystals

Propagation through a heterogeneous photonic crystal stack can be regarded as an alternating sequence of propagation through a uniform layer (Sec. III A) and the diffraction of the field at the common interface of two successive PC layers. Here, we consider the reflection and transmission of Bloch modes at the interface between two semi-infinite media M_1 and M_2, and derive the photonic crystal analogs of Fresnel's reflection and transmission coefficients. The Fresnel coefficients are now Bloch mode scattering matrices, with the domain and range of the transformations defined by the Bloch modes of the input and output media.

The interface between M_1 and M_2 is a fictitious line that is the boundary between a grating layer in each medium. Since all field components are continuous on this line, both the upward and the downward propagating fields must be continuous across the interface. Denoting by $\mathbf{f}_1$ and $\mathbf{f}_2$ the fields (4) on either side of the interface, we can express field continuity by the relation

$$\begin{aligned}\mathbf{f}_1 \overset{\mathrm{def}}{=} \mathcal{F}_1\mathbf{c}_1 = \begin{bmatrix} \boldsymbol{F}_1^- \\ \boldsymbol{F}_1^+ \end{bmatrix}\boldsymbol{c}_1^- + \begin{bmatrix} \boldsymbol{F}_1^{-\prime} \\ \boldsymbol{F}_1^{+\prime} \end{bmatrix}\boldsymbol{c}_1^+ = \begin{bmatrix} \boldsymbol{F}_2^- \\ \boldsymbol{F}_2^+ \end{bmatrix}\boldsymbol{c}_2^- + \begin{bmatrix} \boldsymbol{F}_2^{-\prime} \\ \boldsymbol{F}_2^{+\prime} \end{bmatrix}\boldsymbol{c}_2^+ \\ = \mathcal{F}_2\mathbf{c}_2 \overset{\mathrm{def}}{=} \mathbf{f}_2.\end{aligned} \quad (38)$$

In Eq. (38), the $\mathbf{c}_j^{\mp}$ denote vectors containing the Bloch mode coefficients at the interface in region j. Note that these are the same vectors referred to in the previous section as $\boldsymbol{c}_{\mp}$, now defined for each distinct region j.

We now define the generalized Fresnel (Bloch mode) reflection and transmission matrices by the relations

$$\mathbf{c}_1^+ \overset{\mathrm{def}}{=} \mathsf{R}_{12}\boldsymbol{c}_1^- + \mathsf{T}_{21}'\boldsymbol{c}_2^+, \quad (39)$$

$$\mathbf{c}_2^- \overset{\mathrm{def}}{=} \mathsf{T}_{12}\boldsymbol{c}_1^- + \mathsf{R}_{21}'\boldsymbol{c}_2^+, \quad (40)$$

which express the Bloch modes that are outgoing from the interface in terms of the Bloch modes which are incident on the interface. The Bloch mode scattering matrices are set in a sans serif typeface so as to distinguish them from the plane-wave scattering matrices which are presented in the standard roman typeface. Solving Eq. (38) and expressing outgoing fields in terms of incoming fields then leads to the following expressions for the Bloch mode reflection and transmission matrices:

$$\mathsf{R}_{12} = (\boldsymbol{F}_1^{+\prime})^{-1}(\boldsymbol{I} - \mathbf{R}_2\mathbf{R}_1')^{-1}(\mathbf{R}_2 - \mathbf{R}_1)\boldsymbol{F}_1^-, \quad (41a)$$

$$\mathsf{T}_{12} = (\boldsymbol{F}_2^{-\prime})^{-1}(\boldsymbol{I} - \mathbf{R}_1'\mathbf{R}_2)^{-1}(\boldsymbol{I} - \mathbf{R}_1'\mathbf{R}_1)\boldsymbol{F}_1^-, \quad (41b)$$

where

$$\mathbf{R}_1 = \boldsymbol{F}_1^+(\boldsymbol{F}_1^-)^{-1}, \quad \mathbf{R}_1' = \boldsymbol{F}_1^{-\prime}(\boldsymbol{F}_1^{+\prime})^{-1}. \quad (41c)$$

In Eqs. (41a) and (41b), we see that the domain of each matrix R_{12} and T_{12} is the space spanned by downward propagating modes in M_1, while their range is, respectively, the space of upward propagating modes in M_1 and the space of downward propagating modes in M_2.

Corresponding expressions for R_{21}' and T_{21}' may be obtained from those for R_{12} and T_{12} by transposing the media (i.e., swapping the medium identities denoted by 1, 2), transposing the directionality of the plane waves (i.e., swapping the directions $+,-$), and transposing the directionality of the Bloch modes (i.e., replacing primed quantities by unprimed quantities and vice versa).

In Eq. (41c) $\mathbf{R}_1$ denotes the plane-wave reflection matrix that characterizes reflection of a plane-wave field incident from above on a semi-infinite crystal M_1. The expression for $\mathbf{R}_1$ follows from the consistency condition between incident and reflected plane-wave fields $\boldsymbol{\delta}$ and $\mathbf{r}$ and the downward Bloch modes

$$\begin{bmatrix} \boldsymbol{\delta} \\ \mathbf{r} \end{bmatrix} = \begin{bmatrix} \boldsymbol{F}_1^- \\ \boldsymbol{F}_1^+ \end{bmatrix} \boldsymbol{c}_1^-,$$

which, once $\boldsymbol{c}_1^-$ is eliminated, yields $\boldsymbol{r}=\boldsymbol{F}_1^+(\boldsymbol{F}_1^-)^{-1}\boldsymbol{\delta}$, from which $\mathbf{R}_1$ can be inferred. Correspondingly, $\mathbf{R}_1'$ is the reflection matrix for the same PC, but this time for plane-wave incidence from below.

We turn now to the energy and reciprocity relations satisfied by the Bloch modes to derive corresponding constraints for the generalized Fresnel matrices. In Sec. III A we showed that the flux across an interface (35) is

$$\mathcal{E}_f = \mathbf{c}_1^H \boldsymbol{\mathcal{I}}_1 \mathbf{c}_1 = \mathbf{c}_2^H \boldsymbol{\mathcal{I}}_2 \mathbf{c}_2, \tag{42}$$

provided that the modes are normalized according to Eq. (30b). Here, $\boldsymbol{\mathcal{I}}_m$ is the modal matrix $\boldsymbol{\mathcal{I}}_{\text{BM}}$ [defined in Eq. (30b)], but this time subscripted by m to designate the medium m to which it applies. Expressing $\mathbf{c}_1=[\mathbf{c}_1^{-T}\mathbf{c}_1^{+T}]^T$ and $\mathbf{c}_2=[\mathbf{c}_2^{-T}\mathbf{c}_2^{+T}]^T$ in terms of the modal field $\mathbf{c}_{\text{inc}}$ that is incident on the M_1-M_2 interface, we have

$$\mathbf{c}_1 = \mathsf{U}_1 \mathbf{c}_{\text{inc}}, \quad \mathbf{c}_2 = \mathsf{U}_2 \mathbf{c}_{\text{inc}}, \tag{43a}$$

where

$$\mathbf{c}_{\text{inc}} = \begin{bmatrix} \boldsymbol{c}_1^- \\ \boldsymbol{c}_2^+ \end{bmatrix}, \quad \mathsf{U}_1 = \begin{bmatrix} \boldsymbol{I} & \mathbf{0} \\ \mathsf{R}_{12} & \mathsf{T}_{21}' \end{bmatrix}, \quad \mathsf{U}_2 = \begin{bmatrix} \mathsf{T}_{12} & \mathsf{R}_{21}' \\ \mathbf{0} & \boldsymbol{I} \end{bmatrix}. \tag{43b}$$

After substituting Eqs. (43a) and (43b) into the conservation relation (42) and allowing $\mathbf{c}_{\text{inc}}$ to be arbitrary, we deduce

$$\mathsf{U}_2^H \boldsymbol{\mathcal{I}}_2 \mathsf{U}_2 = \mathsf{U}_1^H \boldsymbol{\mathcal{I}}_1 \mathsf{U}_1. \tag{44}$$

Expanding all four partitions of Eq. (44) and recombining them into a standard form yields the conservation relations summarized by

$$\mathsf{S}^H \mathbf{I}_{12} \mathsf{S} = \mathbf{I}_{12} + i\mathsf{S}^H \mathbf{I}_{\overline{12}} - i\mathbf{I}_{\overline{12}}\mathsf{S}, \tag{45a}$$

where

$$\mathsf{S} = \begin{bmatrix} \mathsf{R}_{12} & \mathsf{T}_{21}' \\ \mathsf{T}_{12} & \mathsf{R}_{21}' \end{bmatrix}, \quad \mathbf{I}_{12} = \begin{bmatrix} \mathbf{I}_1 & \mathbf{0} \\ \mathbf{0} & \mathbf{I}_2 \end{bmatrix}, \quad \mathbf{I}_{\overline{12}} = \begin{bmatrix} \mathbf{I}_{\bar{1}} & \mathbf{0} \\ \mathbf{0} & \mathbf{I}_{\bar{2}} \end{bmatrix}. \tag{45b}$$

Here, S is the S matrix associated with the interface modal reflection and transmission matrices, while $\mathbf{I}_j$ is the identity matrix for real propagating modes in M_j and $\mathbf{I}_{\bar{j}}$ is its complement ($\mathbf{I}_{\bar{j}}=\mathbf{I}-\mathbf{I}_j$) for the evanescent modes in M_j. The result (45) has precisely the same form as the corresponding result (25) for the plane-wave scattering matrices that characterized the reflection and transmission of an individual grating layer. That Eqs. (25) and (45) take exactly the same form is a consequence of correctly normalizing the Bloch modes according to orthogonality relation (30b).

There exists a useful, alternative representation of the result (45) in terms of a Bloch mode transfer matrix $\boldsymbol{\mathcal{T}}_{12}$ that characterizes mode propagation across the M_1-M_2 interface. From Eq. (43a) we have

$$\mathbf{c}_2 = \boldsymbol{\mathcal{T}}_{12}\mathbf{c}_1 \text{ where } \boldsymbol{\mathcal{T}}_{12} = \mathsf{U}_2\mathsf{U}_1^{-1}. \tag{46}$$

The flux conservation relation (42) then implies that

$$\boldsymbol{\mathcal{T}}_{12}^H \boldsymbol{\mathcal{I}}_2 \boldsymbol{\mathcal{T}}_{12} = \boldsymbol{\mathcal{I}}_1, \tag{47}$$

a form which is equivalent to the energy conservation relations in Eq. (45a).

The existence of an energy conservation relation for the interface transfer matrix (45), which is very similar to that for the corresponding plane-wave transfer matrix relationship for a grating layer (23), suggests a modal equivalent of the symplectic property of $\boldsymbol{\mathcal{T}}$ (17). This relation leads us to the reciprocity relations satisfied by the interface reflection and transmission matrices. The reciprocity relations for the interface reflection and transmission matrices follow from the conservation of the skew product $\hat{\mathbf{f}}^T \boldsymbol{\mathcal{Q}}_{\text{PW}} \mathbf{f}$ in Eq. (15), where $\mathbf{f}$ and $\hat{\mathbf{f}}$ correspond to two distinct scattering problems. We define plane-wave scattering quantities $\mathbf{f}_j$ and $\hat{\mathbf{f}}_j$ on either side of the interface ($j=1$, 2). These we express as linear combinations of Bloch modes in terms of Bloch mode coefficients appropriate to the region which, in turn, are expressed in terms of the incident Bloch mode fields (43a). We thus write

$$\mathbf{f}_j = \boldsymbol{\mathcal{F}}_j \mathbf{c}_j = \boldsymbol{\mathcal{F}}_j \mathsf{U}_j \mathbf{c}_{\text{inc}} \text{ and } \hat{\mathbf{f}}_j = \boldsymbol{\mathcal{F}}_j \mathsf{U}_j \hat{\mathbf{c}}_{\text{inc}}. \tag{48}$$

The conservation of the skew-symmetric inner product across the interface thus imposes the condition

$$\hat{\mathbf{c}}_{\text{inc}}^T \mathsf{U}_1^T \boldsymbol{\mathcal{F}}_1^T \boldsymbol{\mathcal{Q}}_{\text{PW}} \boldsymbol{\mathcal{F}}_1 \mathsf{U}_1^T \mathbf{c}_{\text{inc}_i} = \hat{\mathbf{c}}_{\text{inc}}^T \mathsf{U}_2^T \boldsymbol{\mathcal{F}}_2^T \boldsymbol{\mathcal{Q}}_{\text{PW}} \boldsymbol{\mathcal{F}}_2 \mathsf{U}_2^T \mathbf{c}_{\text{inc}}, \tag{49}$$

which implies that

$$\mathsf{U}_2^T \boldsymbol{\mathcal{Q}}_{\text{BM}} \mathsf{U}_2 = \mathsf{U}_1^T \boldsymbol{\mathcal{Q}}_{\text{BM}} \mathsf{U}_1 \quad \text{where } \boldsymbol{\mathcal{Q}}_{\text{BM}} = \begin{bmatrix} \mathbf{0} & \boldsymbol{I} \\ -\boldsymbol{I} & \mathbf{0} \end{bmatrix}, \tag{50}$$

after observing that $\hat{\mathbf{c}}_{\text{inc}}$ and $\mathbf{c}_{\text{inc}}$ may be arbitrary and that the modes in each region are normalized according to the reciprocity relation (30a). Here, $\boldsymbol{\mathcal{Q}}_{\text{BM}}$ is the Bloch mode equivalent operator to the plane-wave form $\boldsymbol{\mathcal{Q}}_{\text{PW}}$, but this time for the Bloch mode basis.

Now expanding all four partitions of Eq. (50) we deduce the reciprocity relations for the generalized Fresnel matrices

$$\mathsf{R}_{12}^T = \mathsf{R}_{12}, \quad \mathsf{R}_{21}'^T = \mathsf{R}_{21}', \text{ and } \mathsf{T}_{12}^T = \mathsf{T}_{21}', \tag{51}$$

which may be simply summarized in the form $\mathsf{S}^T=\mathsf{S}$. Thus, reciprocity implies scattering matrix symmetry, provided that we operate with our basis suitably normalized according to Eq. (30a). Finally, by rearranging Eq. (50), we may obtain an

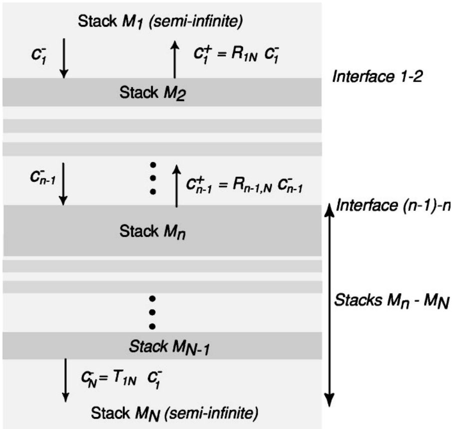

FIG. 3. Recursive coupling of grating stacks. An incident field from above, $\mathbf{c}_1^-$, in semi-infinite stack M_1, is reflected back into $M_1(\mathbf{c}_1^+)$ and transmitted through the N stacks to semi-infinite stack $M_N(\mathbf{c}_N^-)$.

equivalent transfer matrix form of the result, i.e.,

$$\mathcal{T}_{12}^T \mathcal{Q}_{\mathrm{BM}} \mathcal{T}_{12} = \mathcal{Q}_{\mathrm{BM}}. \tag{52}$$

We conclude by observing that the results stated in this section hold to within machine precision since the underlying properties hold within the multipole method that is used to calculate the scattering matrices. It can be shown via a lengthy analysis that these results propagate through the formulation to yield the corresponding results for Bloch mode quantities derived above, independently of any series truncation errors in the calculation of the grating layer plane-wave scattering matrices.

C. Recursive coupling of stacks

The properties of linear devices comprising a sequence of heterogeneous media can be calculated through recurrence relations for the reflection and transmission properties. We outline the process by adding the stack M_n indicated in Fig. 3, thus deriving the Bloch mode scattering matrices $\mathsf{R}_{n-1,N}, \mathsf{T}_{n-1,N}$ from $\mathsf{R}_{n,N}, \mathsf{T}_{n,N}$, where $\mathsf{R}_{n,m}$ and $\mathsf{T}_{n,m}$ represent the Bloch mode reflection and transmission matrices for a stratified structure comprising stacks $M_n, M_{n+1}, \ldots M_m$, for downward incidence in M_n, upward reflection in M_n, and downward transmission in M_m. Now, at the M_{n-1}-M_n interface, we have

$$\boldsymbol{c}_{n-1}^+ = \mathsf{R}_{n-1,n}\boldsymbol{c}_{n-1}^- + \mathsf{T}'_{n,n-1}\boldsymbol{c}_n^+(0), \tag{53a}$$

$$\boldsymbol{c}_n^-(0) = \mathsf{T}_{n-1,n}\boldsymbol{c}_{n-1}^- + \mathsf{R}'_{n,n-1}\boldsymbol{c}_n^+(0). \tag{53b}$$

Similarly, on the upper side of the M_n-M_{n+1} interface,

$$\boldsymbol{c}_n^+(L_n) = \mathsf{R}_{n,N}\boldsymbol{c}_n^-(L_n), \tag{53c}$$

while the transmission into medium M_N is expressed by

$$\boldsymbol{c}_N^- = \mathsf{T}_{n,N}\boldsymbol{c}_n^-(L_n), \tag{53d}$$

where

$$\boldsymbol{c}_n^-(L_n) = \boldsymbol{\Lambda}_n^{L_n}\boldsymbol{c}_n^-(0), \tag{53e}$$

$$\boldsymbol{c}_n^+(0) = \boldsymbol{\Lambda}_n^{L_n}\boldsymbol{c}_n^+(L_n). \tag{53f}$$

Solving Eqs. (53a)–(53f), we derive the recurrence relations

$$\mathsf{R}_{n-1,N} = \mathsf{R}_{n-1,n} + \mathsf{T}'_{n,n-1}\boldsymbol{\Lambda}_n^{L_n}\mathsf{R}_{n,N}\boldsymbol{\Lambda}_n^{L_n} \cdot (\mathsf{I} - \mathsf{R}'_{n,n-1}\boldsymbol{\Lambda}_n^{L_n}\mathsf{R}_{n,N}\boldsymbol{\Lambda}_n^{L_n})^{-1}\mathsf{T}_{n-1,N}, \tag{54a}$$

$$\mathsf{T}_{n-1,N} = \mathsf{T}_{n,N}\boldsymbol{\Lambda}_n^{L_n} \cdot (\mathsf{I} - \mathsf{R}'_{n,n-1}\boldsymbol{\Lambda}_n^{L_n}\mathsf{R}_{n,N}\boldsymbol{\Lambda}_n^{L_n})^{-1}\mathsf{T}_{n-1,N} \tag{54b}$$

with $\mathsf{R}_{n-1,N}$ and $\mathsf{T}_{n-1,N}$ defined according to

$$\boldsymbol{c}_{n-1}^+ \overset{\text{def}}{=} \mathsf{R}_{n-1,N}\boldsymbol{c}_{n-1}^-,$$

$$\boldsymbol{c}_N^- \overset{\text{def}}{=} \mathsf{T}_{n-1,N}\boldsymbol{c}_{n-1}^-.$$

Equations (54a) and (54b) are the means by which we compute the Bloch mode scattering matrices for an entire stack $(\mathsf{R}_{1N}, \mathsf{T}_{1N})$. However, it is theoretically useful to formulate the stack recurrence in terms of transfer matrices. The recurrence relations (54a) and (54b) manifest themselves in transfer matrix form as

$$\hat{\mathcal{T}}_{n-1,N} = \hat{\mathcal{T}}_{n,N}\hat{\mathcal{T}}_{n-1,n}, \tag{55}$$

where $\hat{\mathcal{T}}_{n,N}$ denotes the transfer matrix of the composite structure comprising media $M_n, \ldots, M_N$. The matrix $\hat{\mathcal{T}}_{n-1,n}$, denoting the transfer across the layer bounded by the upper sides of the M_{n-1}-M_n and M_n-M_{n+1} interfaces, is given by

$$\hat{\mathcal{T}}_{n-1,n} = \begin{bmatrix} \boldsymbol{\Lambda}_n^{L_n} & \mathbf{0} \\ \mathbf{0} & \boldsymbol{\Lambda}_n^{L_n} \end{bmatrix} \mathcal{T}_{n-1,n}. \tag{56}$$

Here, $\mathcal{T}_{n-1,n}$ is the transfer matrix associated with the M_{n-1}–M_n interface, while the first matrix in expression (56) is the transfer matrix associated with propagation across the layer.

Accordingly, the transfer matrix for the entire stack is

$$\hat{\mathcal{T}}_{1,N} = \hat{\mathcal{T}}_{N-1,N} \cdots \hat{\mathcal{T}}_{2,3}\hat{\mathcal{T}}_{1,2}, \tag{57}$$

where $\hat{\mathcal{T}}_{N-1,N} = \mathcal{T}_{N-1,N}$. The individual terms of Eq. (57) each satisfy the reciprocity and energy conservation relations (58a) and (58b)

$$\hat{\mathcal{T}}_{n-1,n}^T \mathcal{Q}_{\mathrm{BM}} \hat{\mathcal{T}}_{n-1,n} = \mathcal{Q}_{\mathrm{BM}}, \tag{58a}$$

$$\hat{\mathcal{T}}_{n-1,n}^H \mathcal{I}_n \hat{\mathcal{T}}_{n-1,n} = \mathcal{I}_{n-1} \tag{58b}$$

introduced in the previous section, and thus the combination of Eqs. (57) and (58) implies

$$\hat{\mathcal{T}}_{1,N}^T \mathcal{Q}_{\mathrm{BM}} \hat{\mathcal{T}}_{1,N} = \mathcal{Q}_{\mathrm{BM}}, \tag{59a}$$

$$\hat{\mathcal{T}}_{1,N}^H \mathcal{I}_N \hat{\mathcal{T}}_{1,N} = \mathcal{I}_1. \tag{59b}$$

Realizing that $\hat{\mathcal{T}}_{1,N}$ can be factored as in Eq. (46),

$$\hat{\mathcal{T}}_{1,N} = \begin{bmatrix} \mathsf{T}_{1N} & \mathsf{R}'_{N1} \\ \mathbf{0} & \boldsymbol{I} \end{bmatrix} \begin{bmatrix} \boldsymbol{I} & \mathbf{0} \\ \mathsf{R}_{1N} & \mathsf{T}'_{N1} \end{bmatrix}^{-1},$$

the relationships (59a) and (59b) can be used to establish the symmetry relations

$$\mathsf{R}_{1N}^{T} = \mathsf{R}_{1N}, \quad \mathsf{R}_{N1}'^{T} = \mathsf{R}'_{N1}, \text{ and } \mathsf{T}_{1N}^{T} = \mathsf{T}'_{N1} \qquad (60)$$

and also energy conservation relationships for the stack analogous to those of Eqs. (45a) and (45b). It can be shown that all symmetry and energy conservation relations that hold analytically for each interface and each layer are preserved by the recurrence relations.

Accordingly, this prohibits the use of energy conservation and reciprocity as valid physical tests of the accuracy of the formulation in the case of an implementation in which the grating scattering matrices already preserve these properties analytically. In our case, where the multipole method imbues the entire formulation with such properties, such tests are valuable only insofar as they ensure the correctness of computational implementation. It is therefore important to ensure convergence of the method, which is dependent on the truncation dimensions of plane-wave and modal fields (i.e., the number of evanescent terms included)—the only real means of validating results and comparing them against those obtained by entirely different means. To this end, we have confirmed the accuracy of this method using results obtained from a recently developed Wannier function method [22], demonstrating agreement of results to better than 1 part in 1000.

IV. DISCUSSION AND CONCLUSIONS

We have developed the method in terms of the natural basis of Bloch modes of individual PC layers and have shown that the structure of the formulation closely mirrors that of thin-film optics, with familiar scalar quantities such as Fresnel coefficients being generalized to appropriate matrix forms. While the theory presented here has been developed for 2D structures consisting of uniform cylinders in an otherwise uniform background, and operated in their fundamental polarizations, the analysis extends straightforwardly to handle generalizations. Note that our derivation does not rely on the refractive index distribution in the PC. The only difference is that for more general refractive index distributions the scattering matrices cannot be obtained using the multipole formulation; instead, methods such as those mentioned in Sec. II A need to be used. The theory developed here also extends to vector fields in conical incidence [27]. While the scattering matrices and the form of the reciprocity and energy relationships become more complex, the overall structure of the formulation is then unchanged, as are the essential results concerning modal reciprocity and modal orthogonality.

In developing the theory we have attempted to ensure that the important physical concepts of reciprocity and energy conservation are represented in their most appropriate, convenient, and physically intuitive form. In doing so, we paid particular attention to the formal properties of the Bloch modes and demonstrated key relations: one based on reciprocity, valid even in the presence of loss [Eq. (30a)], and another based on energy conservation, which is valid only in lossless media [Eq. (30b)]. These lead to modal orthogonality and normalization relations which are important in normalizing modes for subsequent calculations involving inhomogeneous media, examples of which are treated in Paper II.

As has been emphasized in Sec. II C, the orthogonality relations derived here are completely different from those associated with the usual Hermitian operator formulation [43] of the eigenvalue problem. Such a treatment [43] begins with a prescibed Bloch vector and generates as its eigenvalues the permissible frequencies of the modes. In our treatment, the starting point is the selection of a frequency, with the eigenparameters being the Bloch vectors and associated Bloch functions. In passing, we observe that the transposition of the role of the eigenparameters makes the method outlined here more amenable to the study of dispersive structures since the initial choice of frequency embeds the optical constants of the materials within the formulation from the outset.

It is interesting also to compare the orthogonality relations derived here with those for the modes of conventional waveguides, such as discussed by Snyder and Love [42]. These authors also identified relations reminiscent of Eq. (30a) that are valid in the presence of loss and an additional relation that holds for lossless media that might be considered to be equivalent to Eq. (30b). As mentioned earlier, the skew-symmetric and Hermitian products in which these relations are cast in our work are directly related to the cross products and scalar triple products in the theory of conventional waveguides.

There are, however, quite distinct differences in the nature of the modes between conventional and photonic crystal waveguides. In lossless media, the complete set of modes in conventional waveguides comprises the bound modes, which are discrete, radiation modes which are continuous, and evanescent modes which are also continuous [42]. Here, the bound modes and radiation modes have real propagation constants β, so that $\exp(i\beta z)$, where z is a propagation distance, always lies on the unit circle, while the evanescent modes have complex propagation constants and correspond to attenuation of the field as the mode propagates along the waveguide.

For a lossless photonic crystal waveguide, all of the various mode classes are discrete, but this is a consequence of the finite size of the periodic supercell geometry, and is not an essential difference from conventional waveguides. A more substantial difference is that when a photonic crystal waveguide structure is operated in a band gap, the mode set comprises both propagating ($|\mu|=1$) and evanescent ($|\mu| \neq 1$) modes. However, the spectrum contains no equivalent of radiation modes, since the band gap guiding mechanism provides for total field confinement—in contrast to leaky total internal reflection which characterizes radiation modes in conventional guides. However, when a PC waveguide is operated in a passband, the modes comprise a set that has the characteristics of conventional radiation modes ($|\mu|=1$) and a set of evanescent modes ($|\mu| \neq 1$). While the modes are again discrete, it can be demonstrated that the number of propagating modes (i.e., with $|\mu|=1$) increases roughly in proportion to the length of the supercell period—a signature that these modes are associated with a continuum of states in the limit when the supercell period approaches infinity.

In our companion article (Part II), which deals with the application of the method to two-dimensional devices, the calculations have relied on the scattering matrices generated by the multipole method [20]. While this is a proven and efficient tool, it has obvious restrictions in terms of the range of structures and geometries that can be handled. Irrespective of this limitation, transfer matrix methods are well suited [27,32] to a wide range of 2D and 3D structures as shown in recent work by Li *et al.* [31,32] who derived efficient and accurate methods for computing the necessary scattering matrices. Accordingly, the key results of this paper concerning both the method and the analytic properties of the modes should readily generalize to 3D. While it is not within the scope of this paper to develop results for fully three-dimensional systems, we nevertheless observe that it is possible to establish results for such systems that are generalizations of Eqs. (15) and (23), and of Eqs. (30a) and (30b), since these particular results follow directly from the underpinning physical considerations of reciprocity and energy conservation. We note here that Eqs. (15) and (30a) follow from reciprocity, a geometrical constraint that does not rely on the material properties of the structure. On the other hand, Eqs. (23) and (30b) follow from conservation of energy and are thus appropriate only to lossless systems. In the case of models of 3D photonic crystal slabs, in which absorbing boundary conditions are needed to isolate adjacent supercells, we would expect to be able to establish the symplectic nature of the transfer matrix but not the orthogonality properties.

Now that the details and the formal properties of the method have been derived, the formulation is ready to be used for solving propagation problems. Such applications of the formalism to a number of different photonic crystal devices are given in Part II.

ACKNOWLEDGMENTS

This work was produced with the assistance of the Australian Research Council under the ARC Centres of Excellence program. We thank Sergei Mingaleev for providing numerical data with which to compare results from the Bloch mode method.

[1] *Photonic Crystals and Light Localization in the 21st Century*, 1st ed., edited by C. M. Soukoulis (Kluwer, Dordrecht, 2001).
[2] A. Mekis, J. C Chen, I. Kurland, S. Fan, P. R. Villeneuve, and J. D Joannopoulos, Phys. Rev. Lett. **77**, 3787 (1996).
[3] T. D. Happ, I. I. Tartakovskii, V. D. Kulakovskii, J. P. Reithmaier, M. Kamp, and A. Forchel, Phys. Rev. B **66**, 041303(R) (2002).
[4] G. Parker and M. Charlton, Phys. World **8**, 29 (2000).
[5] S. John and M. Florescu, J. Opt. A, Pure Appl. Opt. **3**, S103 (2001).
[6] A. Talneau, L. L. Gouezigou, N. Bouadma, M. Kafesaki, C. M. Soukoulis, and M. Agio, Appl. Phys. Lett. **80**, 547 (2002).
[7] S. Boscolo, M. Midrio, and T. F. Krauss, Opt. Lett. **27**, 1001 (2002).
[8] S. Fan, S. G. Johnson, and J. D. Joannopoulos, J. Opt. Soc. Am. B **18**, 162 (2001).
[9] S. Fan, P. R. Villeneuve, J. D. Joannopoulos, and H. A. Haus, Phys. Rev. Lett. **80**, 960 (1998).
[10] S. Boscolo, M. Midrio, and C. G. Someda, IEEE J. Quantum Electron. **38**, 47 (2002).
[11] T. P. White, L. C. Botten, R. C. McPhedran, and C. M. de Sterke, Opt. Lett. **28**, 2452 (2003).
[12] H. Kosaka, T. Kawashima, A. Tomita, M. Notomi, T. Tamamura, T. Sato, and S. Kawakami, Appl. Phys. Lett. **74**, 1370 (1999).
[13] A. Martinez, A. Griol, P. Sanchis, and J. Marti, Opt. Lett. **28**, 405 (2003).
[14] E. Miyai, M. Okano, M. Mochizuki, and S. Noda, Appl. Phys. Lett. **81**, 3729 (2002).
[15] C. T. Chan, Q. L. Yu, and K. M. Ho, Phys. Rev. B **51**, 16635 (1995).
[16] K. M. Leung and Y. F. Liu, Phys. Rev. Lett. **65**, 2646 (1990).
[17] F. Fogli, L. Saccomandi, and P. Bassi, Opt. Express **10**, 54 (2002).
[18] J. B. Pendry, J. Mod. Opt. **41**, 209 (1994).
[19] N. Stefanou, V. Yannopapas, and A. Modinos, Comput. Phys. Commun. **132**, 189 (2000).
[20] L. C. Botten, N. A. Nicorovici, A. A. Asatryan, R. C. McPhedran, C. M. de Sterke, and P. A. Robinson, J. Opt. Soc. Am. A **17**, 2165 (2000).
[21] K. Busch, S. F. Mingaleev, A. Garcia-Martin, M. Schillinger, and D. Herman, J. Phys.: Condens. Matter **15**, R1233 (2003).
[22] K. Busch, S. F. Mingaleev, A. Garcia-Martin, M. Schillinger, and D. Hermann, J. Phys.: Condens. Matter **15**, 1233 (2003).
[23] M. Koshiba, IEICE Trans. Electron. **85**, 881 (2002).
[24] C. Manolatou, S. G. Johnson, S. Fan, P. R. Villeneuve, H. A. Haus, and J. D. Joannopoulos, J. Lightwave Technol. **17**, 1682 (1999).
[25] S. Kuchinsky, V. Y. Golyatin, A. Y. Kutinov, T. P. Pearsall, and D. Nedeljkovic, IEEE J. Quantum Electron. **38**, 1349 (2002).
[26] L. C. Botten, N. A. Nicorovici, R. C. McPhedran, C. M. de Sterke, and A. A. Asatryan, Phys. Rev. E **64**, 046603 (2001).
[27] G. H Smith, L. C Botten, R. C McPhedran, and N. A Nicorovici, Phys. Rev. E **67**, 056620 (2003).
[28] B. Gralak, S. Enoch, and G. Tayeb, J. Opt. Soc. Am. A **19**, 1547 (2002).
[29] S. F. Mingaleev and K. Busch, Opt. Lett. **28**, 619 (2003).
[30] Z. Y. Li and K. M. Ho, Phys. Rev. B **68**, 155101 (2003).
[31] Z. Y. Li and K. M. Ho, Phys. Rev. B **68**, 245117 (2003).
[32] Z. Y. Li and L. L. Lin, Phys. Rev. E **67**, 046607 (2003).
[33] L. C. Botten, A. A. Asatryan, T. N. Langtry, T. P. White, C. M. de Sterke, and R. C. McPhedran, Opt. Lett. **28**, 854 (2003).
[34] L. C. Botten, T. P. White, C. M. de Sterke, R. C. McPhedran, A. A. Asatryan, and T. N. Langtry, Opt. Express **12**, 1592

(2004).

[35] T. P. White, L. C. Botten, C. M. de Sterke, R. C. McPhedran, A. A. Asatryan, and T. N. Langtry, following paper, Phys. Rev. E (to be published).

[36] M. Nevière and E. Popov, *Light Propagation in Periodic Media* (Marcel Dekker, New York, 2003).

[37] *Electromagnetic Theory of Gratings*, edited by R. Petit (Springer, Heidelberg, 1980).

[38] L. C. Botten, N. A. Nicorovici, A. A. Asatryan, R. C. McPhedran, C. M. de Sterke, and P. A. Robinson, J. Opt. Soc. Am. A **17**, 2177 (2000).

[39] M. Hammermesh, *Group Theory and Its Application to Physical Problems* (Addison-Wesley, Reading, MA, 1962).

[40] K. A. Muttalib, J.-L. Pichard, and A. D. Stone, Phys. Rev. Lett. **59**, 2475 (1985).

[41] P. A. Mello and L.-L. Pichard, J. Phys. I **1**, 493 (1991).

[42] A. W. Snyder and J. D. Love, *Optical Waveguide Theory* (Chapman and Hall, London, 1983).

[43] J. D. Joannopoulos, R. D. Meade, and J. N. Winn, *Photonic Crystals: Molding the Flow of Light* (Princeton University Press, Princeton, NJ, 1995).